

HIGH POWER N-TYPE METAL-WRAP-THROUGH CELLS AND MODULES USING INDUSTRIAL PROCESSES

N. Guillevin^a, B.J.B. Heurtault^a, L.J. Geerligs^a, B.B Van Aken^a, I.J. Bennett^a, M.J. Jansen^a, A.W. Weeber^a, J.H. Bultman^a, Wang jianming^b, Wang ziqian^b, Zhai jinye^b, Wan zhiliang^b, Tian shuquan^b, Zhao wenchao^b, Hu zhiyan^b, Li gaofei^b, Yu bo^b, Xiong jingfeng^b

^aECN Solar Energy, P.O. Box 1, NL-1755 ZG Petten, the Netherlands - email: guillevin@ecn.nl

^bYingli Green Energy Holding Co.,Ltd. 3399 North Chaoyang Avenue, Baoding, China.

ABSTRACT: This paper reviews our recent progress in the development of metal wrap through (MWT) cells and modules, produced from n-type Czochralski silicon wafers. The use of n-type silicon as base material allows for high efficiencies: for front emitter-contacted industrial cells, efficiencies above 20% have been reported. N-type MWT (n-MWT) cells produced by industrial process technologies allow even higher efficiency due to reduced front metal coverage. Based on the same industrial technology, the efficiency of the bifacial n-MWT cells exceeds the efficiency of the n-type front-and-rear contact and bifacial “Pasha” technology (n-Pasha) by 0.1-0.2% absolute, with a maximum n-MWT efficiency of 20.1% so far.

Additionally, full back-contacting of the MWT cells in a module results in reduced cell to module (CTM) fill factor losses. In a direct 60-cell module performance comparison, the n-MWT module, based on integrated backfoil, produced 3% higher power output than the comparable tabbed front emitter-contacted n-Pasha module. Thanks to reduced resistive losses in copper circuitry on the backfoil compared to traditional tabs, the CTM FF loss of the MWT module was reduced by about 2.2%abs. compared to the tabbed front emitter contact module. A full-size module made using MWT cells of 19.6% average efficiency resulted in a power output close to 280W.

Latest results of the development of the n-MWT technology at cell and module level are discussed in this paper, including a recent direct comparison run between n-MWT and n-Pasha cells and results of n-MWT cells from 140µm thin mono-crystalline wafers, with only very slight loss (1% of I_{sc}) for the thin cells. Also reverse characteristics and effects of reverse bias for extended time at cell and module level are reported, where we find a higher tolerance of MWT modules than tabbed front contact modules for hotspots.

Keywords: metal wrap through; MWT; n-type silicon; back-contact

1 INTRODUCTION

High efficiency, ease of industrialization and reliability are the main drivers towards low-cost (€/Wp) Silicon PV. The International Technology Roadmap for PV expects the share of rear contact technology to take off rapidly in 2013-2014, and reach 40% in 2020. In accordance with this expected trend, the ECN's n-type Metal-Wrap-Through (n-MWT) technology is a relatively small step from the n-type front-and-rear contact and bifacial Pasha technology (developed by ECN and produced by Yingli under the brand name Panda cells [1]) to a high-efficiency rear-contact cell and module technology which offers significant cell and module performance gain in a cost-effective way [2]. With only modest changes to the n-Pasha production process, the n-MWT technology reproducibly increases the performance: up to 0.3% abs. efficiency gain at cell level and up to 3% power gain at module level have been demonstrated [2] (up to 5% module power gain anticipated). A full size module made using n-MWT cells of 19.6% average efficiency resulted in a power output close to 280W (despite some I_{sc} -mismatch). To place in perspective, with cell efficiency over 20%, a full area n-MWT module efficiency above 18.5% is expected.

ECN's MWT module technology is based on an integrated conductive back-foil and allows to reduce cell-to-module power loss compared to a conventional tabbing technology, as used to interconnect the n-Pasha cells. Also, the module manufacturing based on integrated back-foil can be done with higher yield and reduced interconnection-process-related stress, allowing use of (much) thinner cells and therefore offering additional cost reduction possibilities. Our latest results in this paper therefore include wafers of varying thickness. In addition to efficiency and cost improvements, module reliability is important. One of the technical requirements of PV

modules according to the standard IEC61215 is to pass the hot spot endurance test. Higher cell efficiencies in combination with a trend towards 72-cell modules tend to increase power dissipation in hot spots, if those occur. Consequently, thorough investigation of cell and module reverse current characteristics must be part of the industrialization process.

In this paper, the latest results of the n-MWT technology development will be discussed. In a recent direct comparison run between n-MWT and n-Pasha, a 0.15%abs. efficiency gain was obtained for n-MWT over n-Pasha and a best efficiency of 20.1% was obtained on n-MWT (in-house measurement). Since back contact module technology allows the use of very thin cells, comparison of n-MWT cells of varying thickness is relevant: processing of n-MWT cells from thin mono-crystalline silicon Cz wafers down to 140µm (before texturing process) was therefore investigated. Only a small loss (1% of I_{sc}) was found for the thin cells, in principle not even significant within the experimental scatter, but in agreement with cell modeling.

In addition to the latest cell results and effect of wafer thickness, focus will be on reverse characteristics of the n-MWT cells and on module reliability aspects. Efficiency and reverse characteristics, compared between the n-Pasha and n-MWT technologies, will be described in more detail. Potentially adverse effects of leakage current on n-Pasha and n-MWT single-cell laminates were investigated for a range of reverse currents. Distribution of power dissipation under reverse bias voltage and effect of leakage current in n-MWT cells were investigated by thermal imaging and direct reverse current measurement. Attention was paid to possible instability of cell parameters after prolonged reverse bias in light of recent reports on this effect [3], which we found to be not severe. Interestingly, also, MWT modules were found to be more tolerant to a given level of

leakage current under reverse bias than front contact tabbed modules.

2 MWT CONCEPT FOR N-TYPE MATERIAL

a. Benefits of combining MWT technology with n-type material

MWT technology presents several advantages over the standard H-pattern cell technology. Apart from the current gain due to reduced front-side metallization coverage, integration into a module is easier as the cell is fully back-contacted. The mechanical stress induced on the cells by conductive adhesive based interconnection (used in our MWT modules) is low, and as a result, the breakage is reduced. Consequently, thinner and larger cells can be interconnected without yield loss. In addition, the packing density can be significantly increased. The front side metal grid benefits from a small unit cell pattern allowing large cells (cf. fig. 1). The cell interconnection can be optimized for low series resistance losses and significantly reduced efficiency loss from cell to module, since the constraints related to normal front-to-back tabbed interconnection (i.e., shading loss from the width of tab, and stress on the cell) are absent [4].

In addition to the efficiency enhancement due to MWT layout, efficiency can be increased using silicon base material with improved electrical properties. In that respect, n-type wafers generally allow (much) higher lifetimes than p-type wafers [5,6]. In contrast to boron-doped p-type material, boron-oxygen complexes are absent in n-type material. Therefore it will not suffer from lifetime degradation due to formation of a boron-oxygen related metastable defect upon illumination [7,8]. Also, n-type silicon has been proven to have a higher tolerance to common transition metal impurities [9,10,11]. In practice, lifetimes of several milliseconds are readily obtained in n-type Cz. The n-Pasha cells developed by ECN, Yingli Solar and Amtech (and daughter company Tempres) and brought into production by Yingli Solar, use the conventional non back-contact H-pattern cell structure [1]. In addition to benefiting from high base diffusion length, this cell design has other advantages, in particular, significantly improved rear side optical and electrical properties, compared to standard p-type cells. So far, best cell efficiency of 19.49% (independently confirmed by Fraunhofer ISE) in trial production [11,12] and 20.1% in production have been reached. Recently, efficiencies of 20.2% were obtained at ECN's pilot line on high quality n-Cz material [13].

MWT cell process technology in general remains close to conventional front contact cell processing, and the simplicity of the rear-side contact pattern of the MWT cells allows large tolerance regarding print alignment. The cell structure comprises a front side emitter and therefore will be less sensitive to material quality variations than back-contact back-junction cell designs. Also, integrated MWT cell and module technology has already proven itself for p-type technology.

b. Approach to cell process development

The n-type MWT process is very similar to the industrial process used for n-Pasha cells. Laser processing is used to form via-holes by which the front side metal grid is wrapped through the wafer. Like the n-Pasha cells, the cell structure comprises a boron emitter, a phosphorous Back Surface Field (BSF) and an open rear side metallization suitable for thin wafers. Metal contacts are deposited by industrial screen-printing process with no

further requirements regarding alignment compared to the screen-printing process used in the industrial n-Pasha process. The front and rear side metal grid patterns are based on a H-pattern lookalike grid design, combined with the unit cell concept [14]. We have chosen a H-pattern lookalike grid because it is well suited for a comparison of losses between n-MWT and n-Pasha cells. As module interconnection of n-MWT cells does not require tabs on the front of the cells, the front side busbars can be significantly slimmed down compared to conventional n-Pasha cells. As a result, total shading losses are reduced. Correspondingly, however, resistance in the busbars affects the total series resistance of the cell. Shading and resistance losses are balanced to increase power output of the n-MWT cells compared to the n-Pasha cells. The front and rear sides of the cells made according to this process sequence can be seen in Figure 1.

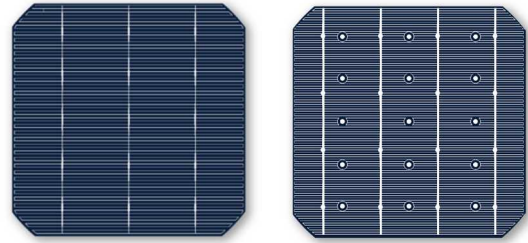


Figure 1. Image of n-type MWT silicon solar cells (239cm^2) with a H-pattern based unit cell design: front side (left picture) and rear side (right picture).

3 N-TYPE MWT VERSUS N-TYPE PASHA CELLS – DIRECT PERFORMANCE COMPARISON

a. Experimental results and analysis – n-MWT vs. n-Pasha

n-type MWT and n-type Pasha solar cells were prepared from $200\ \mu\text{m}$ thick and neighboring n-type Cz wafers ($239\ \text{cm}^2$, around $1.7\ \Omega\text{cm}$ resistivity). Both groups were processed in parallel and received identical texture (random pyramids formed by alkaline etching), emitter and BSF profiles, passivation, SiN_x anti-reflective coating (ARC), metal paste for emitter and BSF contacts and firing. I/V data are presented in Table 1.

Table 1. I/V characteristics of n-type Pasha cells and n-type MWT cells (continuous light source), with comparable J_0 and metallization parameters, to illustrate the gains associated with MWT design. ESTI calibrated reference cell ($2\% I_{sc}$ uncertainty). R_{se} obtained from fit to two-diode model. J_{sc} corrected for spectral mismatch. N-type Pasha and n-type MWT measurement chucks have a reflective surface to simulate the operation in a module with white back sheet. (* indicates FF overestimated due to shorting of the n-Pasha rear grid on the electrically conductive measurement chuck.)

	J_{sc} (mA/cm^2)	V_{oc} (mV)	FF (%)	η (%)	R_{se} ($\text{m}\Omega$)
Av. on 12 cells					
n-Pasha	38.90	652	78.4*	19.89	4.9
n-MWT	39.95	652	76.8	20.04	5.7
Best efficiencies					
n-Pasha	38.97	653	78.5*	19.98	4.8
n-MWT	40.01	653	77.0	20.10	5.6

The J_{sc} gain of 2.6% for the n-MWT cells is related to the reduced front metal shading losses thanks to the narrower front busbars. Because the n-Pasha process used non-contacting front busbar paste, front surface recombination below the large n-Pasha busbar is reduced [1]. Consequently, in contrast to previously reported results [2], no V_{oc} gain related to reduced metal recombination is obtained.

Even with a lower FF, a resulting efficiency gain of 0.15% absolute is measured on the back-contacted cells compared to the H-pattern cell. Contributions to series resistance and FF losses are summarized in Table 2.

Table 2. Calculated contributions to series resistance and FF losses of the n-MWT cells compared to the n-Pasha cells.

Source of R_{series} in MWT cell	R_{series}	FF loss
Metal via resistance	0.2 m Ω	0.3% abs.
Front side busbars	0.7 m Ω	1.1% abs.
Increase of I_{sc}		0.1% abs.
Total	0.9 m Ω	1.5% abs.

From the results in Table 2, approximately 1.5% additional FF loss present in the n-MWT cells, compared to n-Pasha cells, can be explained. The discrepancy between model and experiment is small compared to measurement and modeling uncertainties. In particular the FF measurement of an n-Pasha type cell is quite dependent on experimental configuration.

b. Solutions to reduce series resistance of n-MWT cells and increase efficiency

Several options exist to reduce the FF loss of n-MWT cells relative to n-Pasha cells. A straightforward option is increasing the number of vias [15]. As illustrated in Figure 2, when the number of via-holes increases, FF and J_{sc} increase thanks to the reduction of resistive and shading losses (dashed black and solid blue lines). However, this may also increase recombination, and therefore, cause V_{oc} loss (dotted blue line in Fig. 2). From modeling we expect a maximum efficiency increase of around 0.2% absolute compared to the current number of via-holes.

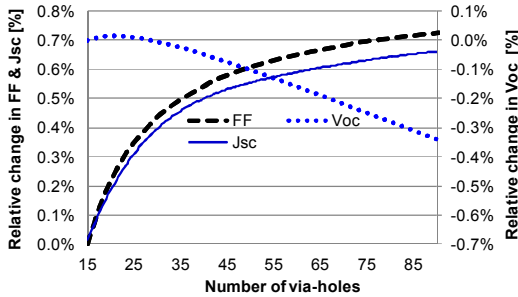


Figure 2. Calculated relative FF, shading and V_{oc} changes as a function of the number of via-holes for n-MWT cells.

4 N-TYPE MWT VERSUS N-TYPE PASHA MODULES DIRECT PERFORMANCE COMPARISON

a. Initial results

The ECN module manufacturing technology used to interconnect the n-MWT cells is based on an interconnection foil with integrated Copper conductor layer, on which the cells are electrically contacted using a conductive adhesive. Compared to the front to rear side tabbed interconnection used for the n-Pasha cells, a rear-side foil interconnection allows to reduce the module series resistance by using more interconnect metal (more cross-sectional area) and thereby reduce the cell to module FF loss.

N-MWT and n-Pasha 60-cells modules were manufactured from cells prepared as described in the previous section (neighboring n-type Cz wafers, 200 μ m thickness, 239cm², and parallel processing). However, because the cells were fabricated further back in time, the process parameters used were not as optimum as they currently are. As a result, average efficiencies of n-MWT and n-Pasha cells are lower than they are today. N-MWT and n-Pasha modules were measured at ECN using a class A multflash tester (8-flash measurement). Average cell efficiency, maximum power and absolute FF loss from cell to module (CTM) are presented in Table 3. The n-MWT module outperforms the corresponding n-Pasha tabbed module with a power gain of 8 Wp and a CTM FF loss of only 0.8% which is more than 3 times lower than the FF loss for n-Pasha.

Table 3. n-type MWT and n-type Pasha average cell efficiency, corresponding module power and FF loss from cell to module (multi-flash class A, IEC60904-9 measurement, ESTI reference module).

	Average cell η	P_{max} (W)	cell-to-module FF loss
n-MWT module	18.9%	273	0.8%
n-Pasha module	18.6%	265	3%

The reflectivity of the back-foils used for the n-MWT module is much lower than the standard TPT back-foil used for the n-Pasha tabbed module. Therefore, significant gain (on the order of 1%) in I_{sc} is possible for n-MWT modules by employing high reflectance back-foils. Fig. 3 illustrates a first step towards a back-foil with improved reflectance, which results in at least 0.5% gain in I_{sc} .

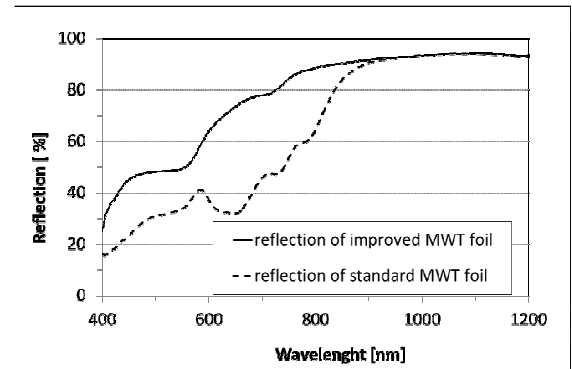


Fig. 3. Reflection measured in air of standard MWT integrated back-foil (used in experiment of Table 3) and a preliminary improved back-foil.

b. Intermediate n-MWT cell & module power improvement

In the period between the fabrication of first n-MWT module and the latest results discussed in section 3, a batch of 60 n-MWT cells were fabricated according to an improved process [1]. This process being less optimal than it is today, the average cell efficiency presented in Table 4 is somewhat lower than the one presented in section 3. The n-MWT cells were prepared from 200 μ m thick n-type Cz wafers (239 cm²). Interconnection of the 60 n-MWT cells was done using the ECN module manufacturing technology as described in section 4a. For this n-MWT module, back sheet with improved reflectivity (fig. 3) was used. The n-MWT module I-V parameters were measured at ECN using a class A multiflash tester (16-flash measurement). Maximum power and absolute FF loss from cell to module are also presented in Table 4.

Table 4. n-type MWT average cell efficiency, corresponding module power and FF loss from cell to module (multi-flash class A, IEC60904-9 measurement, ESTI reference module).

n-MWT module	Average cell η	P_{max} (W)	cell-to-module FF loss
n-MWT module	19.6%	279	1.3%

Despite an improved maximum power, this n-MWT module shows a slightly higher CTM FF loss compared to the n-MWT module presented in section 4a which is possibly due to the use of a different conductive adhesive. Also, the module I_{sc} turned out to be lower than expected from results on earlier modules, because of I_{mpp} mismatch of a few n-MWT cells. With better I_{mpp} matching, the CTM FF-loss of Table 3 and cell efficiency above 20% as demonstrated in section 3, module power above 290Wp is within reach.

5 PROCESSING OF 140 μ M THIN N-MWT CELLS

In addition to the reduced cell-to-module power loss, the ECN's MWT module technology distinguishes itself by its reduced interconnection-process-related stress, allowing use of thinner cells and therefore offering additional cost reduction possibilities. In order to verify the possibility to benefit from this, 140 μ m n-type Cz wafers were processed into n-MWT cells together with the cells described in section 3. Unfortunately, wafers of standard thickness (200 μ m) from identical material (i.e., from a nearby position in the same ingot) were not available. However, a batch of standard thickness wafers (200 μ m) with similar electrical properties (bulk lifetime and diffusion length) was processed in parallel also into n-MWT cells. Average I/V data are presented in Table 5.

Table 5. I/V characteristics of n-type MWT cells processed from 200 μ m and 140 μ m thin wafers (continuous light source). ESTI calibrated reference cell (2% I_{sc} uncertainty). Rse obtained from fit to two-diode model. J_{sc} corrected for spectral mismatch.

	J_{sc} (mA/cm ²)	V_{oc} (mV)	FF (%)	η (%)	R_{sc} (m Ω)
Av. on 12 cells					
n-MWT-200 μ m	39.95	652	76.8	20.04	5.7
n-MWT-140 μ m	39.63	651	76.5	19.74	5.8

There was no increased breakage rate observed during the processing of the thin MWT cells at ECN. Comparable V_{oc} and FF show that there is no significant shift between bulk and surface recombination. A \approx 1% relative lower J_{sc} for the thin n-MWT cells is probably due to reduced light trapping. This effect is illustrated by the higher total reflectance measured in the long wavelengths and shown in figure 4. This higher escape reflectance results from a lower light trapping which also correlates with the lower IQE of the thin n-MWT cell starting from the wavelength of 1000nm (effect from rear internal reflection <100%). These results are consistent with PC1D modeling of our cells. However, we note that fluctuations of 1% in J_{sc} between cells from nominally good material quality can occur anyway, even for standard thickness wafers. Therefore it is difficult to draw firm conclusions on the effect of wafer thickness on J_{sc} at this moment.

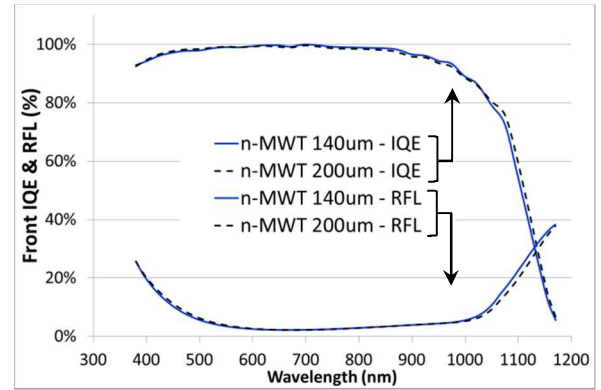


Fig. 4. Internal quantum efficiency and Reflectance measured from the front side of n-MWT cells processed from 200 μ m and 140 μ m wafer thickness.

6 REVERSE CHARACTERISTICS OF N-MWT CELLS AND MODULE

a. Stability of the dark reverse I/V characteristics of the n-MWT cells

The reverse characteristics in the dark of our n-MWT cells are normally very satisfactory (well below 0.5A). Since there have been reports about instability of cell parameters after reverse biasing [3] in this section we present results on the stability of cell characteristics in some detail.

Four n-MWT cells with different initial values of reverse current (I_{rev}) were selected (0.1A, 0.5A, 1A and 9A at -12V) to study stability of the reverse characteristics in dark. Each cell was exposed to a reverse voltage of 12V in the dark for up to one hour. Electro-luminescence images as well as dark I/V characteristics both in reverse voltage bias were acquired at regular time lapses. In this initial study, the cells were placed in the dark on a metal chuck (without active cooling system but with large thermal mass). This is not fully representative for the conditions in the field regarding temperature fluctuations as the metal chuck by itself is most likely a better heat dissipater than the conductive back sheet foil used in an MWT module. However, results of a similar study performed on single-cell laminates are described in the next section.

Figure 5 shows an example of an electro-luminescence measurement under reverse bias performed on an n-MWT cell with high I_{rev} characteristics (9A at -12V). When exposed to a reverse bias voltage of 12V, the current flows

through a (non-linear) shunt or junction breakdown resulting in light emission in the visible wavelength range [16]. The light intensity is proportional to the level of reverse current. As visible in figure 5, particularly on the zoom-in, intense light escapes from the rear-side metal pad edges. This indicates that the high reverse current for this MWT cell originates from a shunt or junction breakdown located at the interface between the metal pad, connected to the front side grid, and the n-type base silicon area around the via-hole which is un-diffused. The type of shunt or junction breakdown has not been identified yet. In the case of low reverse current n-MWT cells (<0.5A at -12V), no emitted light is visible when exposed to a reverse voltage of 12V.

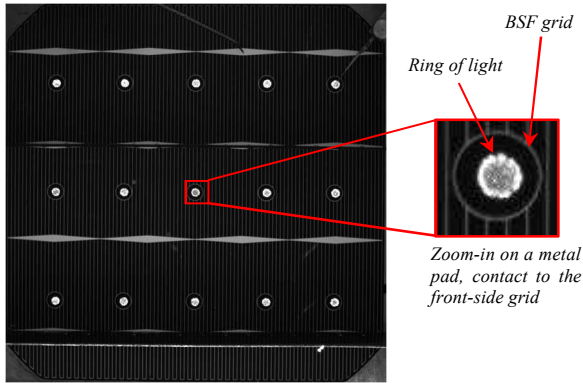


Fig. 5. Grey scale electro-luminescence image of the rear-side of a high I_{rev} n-MWT cell (9A at -12V) under 12V reverse voltage bias. The rear side includes 15 metal pad-contacts to the front side grid (through the via-holes) and 16 diamond-shaped contacts to the base. A zoom-in centered on a metal pad is presented at the right side of the main picture where a ring of light around the metal pad is clearly visible.

Relative changes of I_{rev} level measured at -12V for one hour of exposure at a voltage load of -12V are shown in figure 6. Relative changes of I_{rev} are plotted for the four selected n-MWT cells. From these measurements, two different behaviors independent from the initial I_{rev} values of the cell can be distinguished. For some cells, the reverse current level remains stable over time and can even slightly decrease (case of the cells with initial reverse current of 1A and 0.5A at -12V). For other cells, the reverse current increases within the first 10 minutes to subsequently slightly decrease and stabilize (case of the cells with initial I_{rev} of 9A and 0.1A at -12V). Despite the large relative reverse current increase of 110% measured for the cell with 0.1A initial I_{rev} , its I_{rev} level remains below 0.2A after stabilization. Because absolute reverse current fluctuations under reverse bias remain small, no changes in the electro-luminescence images were detected.

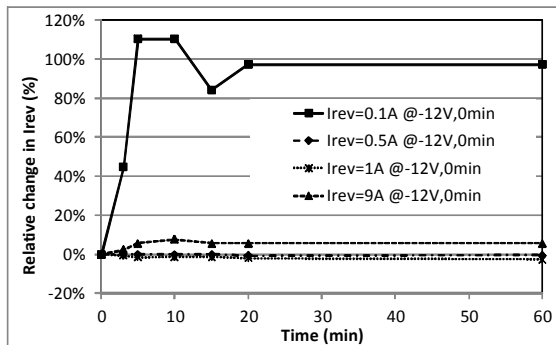


Fig. 6. Relative changes of dark reverse current measured at -12V as a function of exposure time under a reverse voltage of 12V for

four n-MWT having different initial reverse current values (0.1A, 0.5A, 1A and 9A at -12V).

Dark reverse current characteristic as a function of reverse voltage bias are plotted in figure 7 for the two cells showing an increase of I_{rev} level when a bias voltage of -12V is applied (i.e. cells with initial reverse current of 0.1A and 9A at -12V). For both cells, after long exposure to a reverse voltage bias, no dramatic changes in the shape of the I_{rev} curve is visible. The slope at 0V increases to stabilize after 5 minutes of exposure at -12V. In the case of the high reverse current cell (9A at -12V), the high slope degree at 0V corresponds to the low shunt resistance measured in forward bias. Consequently, it appears that fairly high initial I_{rev} can also affect the performance of the cell in forward operation (as reported in [3]). For Fig 7b, within the noise (not shown) there is no noticeable change of slope at zero voltage.

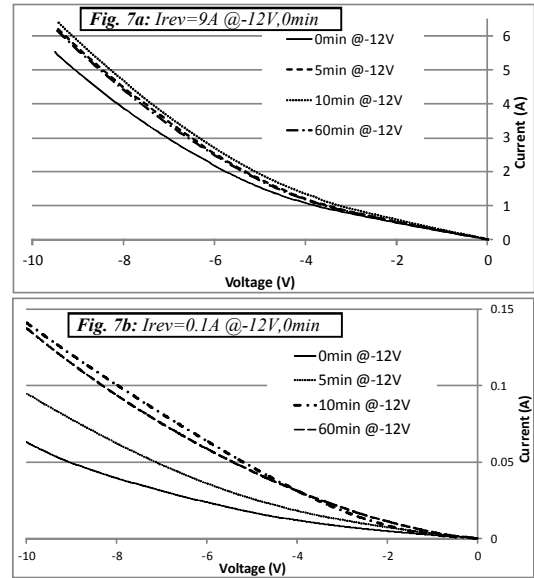


Fig. 7a & 7b. Dark reverse current curves as a function of reverse voltage bias plotted for different exposure time at a voltage load of -12V. Dark reverse current curves are shown for two n-MWT cells: with a high initial I_{rev} (9A at -12V – fig. 6a) and low initial I_{rev} (0.1A at -12V – fig. 6b).

In contrast to the dark I/V characteristics measured on MWT test structure reported by [3] on n-type base material, no sharp current breakdown at low reverse voltage bias is observed on ECN’s MWT cell in the case of “high I_{rev} ”. To prevent potentially adverse effects of reverse current, processing of ECN’s MWT cells is optimized to keep I_{rev} below 0.5A at -12V. Also, independently from the initial reverse current level, no influence of the prolonged exposure at reverse voltage on the forward I/V characteristics was observed.

b. Effect of reverse current in n-MWT and n-Pasha single-cell laminates

Effect of leakage current in n-MWT and n-Pasha laminates is investigated by thermal imaging as described in [17]. Degradation of the laminates was assessed by visual appearance and by the I/V power output. The laminates were exposed to a reverse voltage of 10V for up to one hour in the dark at a base temperature of 50°C.

N-MWT and n-Pasha cells with I_{rev} ranging from 0.5A to 8A were selected. These cells were selected to have

representative hot spot patterns as identified by voltage modulated lock-in thermography (VoMoLIT). Example of VoMoLIT of n-MWT and n-Pasha cells and IR images of the corresponding n-MWT and n-Pasha laminates with I_{rev} of 2.5A are shown in Figure 8. Typically in n-Pasha cells one or two single hot spots or lines are visible. In contrast, in n-MWT cells, the current may flow mainly through the via-holes as also shown in figure 5 (although of course also patterns as for the n-Pasha cell may be present).

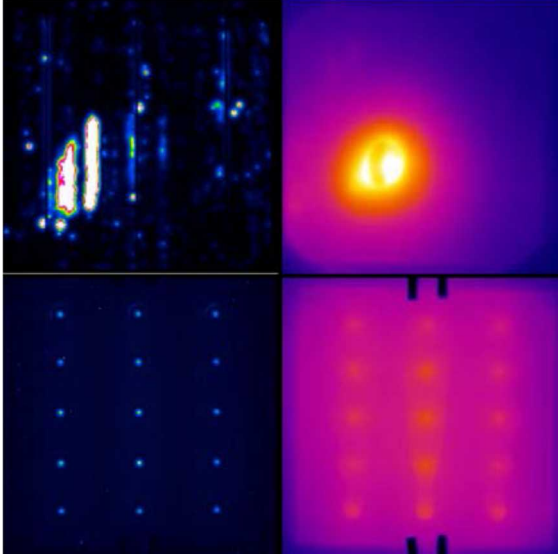


Figure 8. VoMoLIT (left - cell) and IR (right - corresponding laminate) images of samples with I_{rev} of $\approx 2.5A$ at $-10V$, showing n-Pasha(top) and n-MWT (bottom). The temperature scale for the VoMoLIT and IR images are identical. The IR scale ranges from $40^{\circ}C$ (black) to $160^{\circ}C$ (white).

“Hot spot” tests performed on n-MWT and n-Pasha cell with a reverse current above 4A at $-10V$ reveal that temperatures higher than $150^{\circ}C$ are reached for both cell types within few minutes resulting in severe failure of the laminates: the glass is fractured, the back sheet blisters or the surface of the solar cell becomes discoloured. Despite the modest power output decrease of up to 3%, these laminates would fail the IEC criteria.

Significant behaviour differences is observed between n-MWT and n-Pasha laminates assembled with cell with a reverse current lower than 4A. Typical results of the reverse current tests of these laminates are summarized in Table 6. Two cells and corresponding laminates with $I_{rev} \approx 2.5A$ are displayed in the VoMoLIT and IR images of figure 8. Whereas the hotspot feature of the n-Pasha cell is translated to a large hot spot in the laminate reaching a temperature of the back sheet above $160^{\circ}C$, the MWT cell shows only moderately heated via-holes with a temperature below $105^{\circ}C$.

The data in table 6 shows that for $I_{rev} < 4A$, the MWT laminate exhibits a lower maximum temperature. A reverse current of 1.3A is sufficient for this n-Pasha laminate to reach the same temperature of $105^{\circ}C$ as the MWT laminate with a reverse current of 3.1A. A reverse current of 2.6A is sufficient to cause visual damage on the n-Pasha laminate and an efficiency loss of 2% while the n-MWT laminate with 3.1A reverse current remains undamaged.

Table 6. Reverse current (I_{rev}), maximum observed temperature (T_m) and change in power output ($\Delta\eta$) of three laminates.

Laminate type	I_{rev} @-10V (A)	T_m ($^{\circ}C$)	$\Delta\eta$ (%)	Visual failure
n-Pasha	2.6	$>160^{\circ}C$	-2	Yes
n-MWT	3.1	105	-0.02	No
n-Pasha	1.3	110	-0.05	No

As the power dissipation $P=VI$ in all laminates is proportional to I_{rev} , the magnitude of the power dissipation cannot explain the observed differences in temperature between n-MWT and n-Pasha laminates. Figure 8 clearly shows the differences in current flow patterns than can occur between n-MWT and n-Pasha laminates when a reverse voltage bias is applied. For this n-Pasha laminates the current flows mainly through a single spot while in this n-MWT laminates the current is divided over all via-holes. As a consequence the power dissipation in the n-Pasha laminates is concentrated, causing the temperature to reach damaging levels when $I_{rev} > 2A$ while it is distributed in the n-MWT laminates which limits the maximum temperature for the same power dissipation. Furthermore, the full copper back foil used to interconnect the n-MWT cells is likely to help the heat dissipation. Thus, in addition to the magnitude of the current that flows under a reverse voltage, the distribution of this leakage current and means of heat dissipation are also important. In this respect it is necessary to further study the effect of a copper back-foil on the heat dissipation by hot spot patterns typical for n-Pasha cells (which may also occur in n-MWT cells).

7 CONCLUSION

We have developed a manufacturing process for metal-wrap-through silicon solar cells and module on n-type mono-crystalline Czochralski (Cz) silicon wafers, leading to a module power, so far, of 279Wp from cells of 19.6% average efficiency. With current density (J_{sc}) of about 40 mA/cm^2 and open circuit voltages above 650 mV, the large area (239 cm^2) n-MWT solar cells outperform n-Pasha solar cells (bifacial n-type H-pattern cells with contact grids on front and rear) manufactured with a comparable process. In a recent direct comparison experiment, an efficiency gain of 0.15% absolute for MWT was achieved with a best MWT cell efficiency of 20.1%.

Performance enhancement at module level is obtained thanks to the ECN MWT module manufacturing technology based on integrated back-foil (conductive interconnect patterns integrated on the backfoil). In a full size module (60 cells) comparison experiment between MWT and equivalent n-Pasha tabbed modules, a power increase of approximately 3% for the n-MWT module was obtained. Interconnection of a batch of cells with average efficiency of 19.6% resulted in a module power close to 280Wp. Module power gain above 290Wp is expected to be reached by better I_{mpp} matching, further optimization of the back-sheet reflectivity and of course by use of cells with efficiency above 20%.

Successful processing of $140\mu\text{m}$ thin n-MWT cells was demonstrated: low breakage rate (similar to standard thickness cell processing), and a small J_{sc} loss of 1% compared to standard thickness n-MWT cells. This small J_{sc} loss, as well as IQE and reflection measurements, match PC1D modeling of lower light coupling inherent to the wafer thickness. These results together with the low interconnection stress of the ECN’s MWT technology add

another possibility to reduce cost of the technology.

Stability of the dark reverse as well as illuminated I/V characteristics of n-MWT cells after prolonged reverse bias voltage was found to be satisfactory, independently from the level of initial reverse current. Despite a brief rise of the reverse current in the first minutes of reverse bias in some cases, stability is rapidly reached. Reverse voltage in MWT-back contact modules typically causes less thermally-induced damage than in n-Pasha modules with similar I_{rev} , thanks to more optimum distribution of the power dissipation over the via-holes (if those are the main leakage locations) and dissipation by the metal back-foil. This latter benefit needs to be investigated further.

7 ACKNOWLEDGMENTS

This work has been partially funded by AgentschapNL within the International Innovation program under the grant agreement no. OM092001 (Project FANCY). Also part of the research leading to these results has received funding from European Union Seventh Framework Program (FP7-ENV-2012-two-stage) under grant agreement n° 308350. We also gratefully acknowledge collaboration with Tempres Systems.

8 REFERENCES

- [1] I.G. Romijn et al., 27th EU-PVSEC, 2012
- [2] N. Guillevin et al., 27th EU-PVSEC, 2012
- [3] E. Lohmüller et al, 27th EU-PVSEC, 2012
- [4] M.W.P.E. Lamers et al, Proc. 25th EU-PVSEC, 2010, p.1417.
- [5] S. Martinuzzi et al., Pogr. Photovolt.: Res. Appl., 2009, 17: p. 297.
- [6] A. Cuevas et al., Appl. Phys. Lett. 2002, 81: p. 4952.
- [7] J. Schmidt et al., Proc. 26th IEEE PVSC, 1997, p. 13.
- [8] S. Glunz et al., 2nd WCPEC, 1998, p. 1343.
- [9] D. Macdonald and L.J. Geerligts, Appl. Phys. Lett., 2008, 92: p. 4061.
- [10] J.E. Cotter et al., 15th Workshop on Crystalline Silicon Solar Cells & Modules, 2005, p. 3.
- [11] Yingli press release Oct 20, 2010, obtained in trial production lines. Independently verified at ISE.
- [12] Yingli press release Feb 18, 2011. Best efficiency in production lines.
- [13] I.G. Romijn, Industrial n-type solar cells with >20% cell efficiency, CPTIC SolarCON Shanghai, 2013
- [14] A.R. Burgers et al., Solar Energy Materials & Solar Cells, 2001, 65: p. 347.
- [15] N. Guillevin et al, CPTIC SolarCON Shanghai, 2012.
- [16] Obeidat et al., Appl. Phys. Lett., Vol. 70, No. 4, 27 January 1997
- [17] M.J. Jansen, PVSEC-22 Photovoltaic Science and Engineering Conference, Hangzhou, China, , 5-9 November 2012.